Journal of Fluorescence, Vol. 7, No. 4, 1997

Donor–Donor Energy Migration (DDEM) for Determining Intramolecular Distances in Proteins. II. The Effect of Partial Labeling

Jan Karolin,[1] Peter Hägglöf,[2] Tor Ny,[2] and Lennart B.-Å. Johansson[1,3]

Received October 27, 1997; accepted December 4, 1997.

By using site-specific mutagenesis it is possible to prepare a protein molecule that can be labeled with two *identical* fluorescent probes at different positions.[1,2] To calculate intramolecular distances between the two fluorescent donors in a protein, a recently developed DDEM model can be applied.[3,4] Here we have studied the influence of incomplete donor labeling on the calculated distances. For this purpose, the previous model has been extended and compared with experiments performed on three mutants (V106C, M266C, and V106C-M266C) of plasminogen activator inhibitor type 1 (PAI-1) labeled with *N*-(4,4-difluoro-5,7-dimethyl-4-bora-3a,4a-diaza-*s*-indacene-3-yl)methyl) iodo-acetamide (SBDY). The C_α of the residues to which the SBDYs are covalently linked are separated by 55.1 Å, as determined by X-ray diffraction on the wild-type PAI-1. To examine the reliability of the extracted parameters, synthetic data were generated and reanalyzed with the same model as used to analyze real experiments. It is concluded that, even for a low degree of labeled double mutant (≈60%), a distance of 54 ± 3 Å is found for both models.

KEY WORDS: Donor–donor energy migration; intramolecular distance; proteins; partial labeling.

INTRODUCTION

The Förster mechanism of electronic energy transfer[5] has been studied and applied in a large number of reports. According to Förster, the rate of energy transfer (ω) between the donor (d) and the acceptor (a) molecules separated by a distance R is proportional to $1/R^6$. Since the rate of energy transfer depends on the distance between the interacting molecules, one obvious application would be as a spectroscopic ruler. To examine the process of energy transfer, several bichromophoric *da* systems have been synthesized.[6–12] In order to apply *da* transfer to measuring distances in proteins, the *d* and *a* molecules must be *specifically* attached at two sites. In practice, this is an extremely difficult task. For protein labeling, the amine and thiol groups are most commonly used to react with specific fluorescent reagents.[13,14] Since the amine groups are present in several amino acids and in a terminal residue position, they are not suitable for specific labeling. Even if a stochiometric labeling ratio is obtained, the exact localization of the chromophores is usually unknown.[15] In contrast the thiol-reactive probes are very specific for cysteine residues (Cys), which are not as common as the amine group. By using site-directed mutagenesis, a protein can, in principle, be modified to contain only *one* or *two* Cys residues at specific positions. Hence, it is possible to prepare a bichromophoric protein containing two fluorophores of the *same* kind located at specific positions. Further, if the photophysical properties of the probes are independent of their local environment, the energy trans-

[1] Department of Physical Chemistry, Umeå University, S-901 87 Umeå, Sweden.
[2] Department of Medical and Biochemistry, Umeå University, S-901 87 Umeå, Sweden.
[3] To whom correspondence should be addressed.

1053-0509/97/1200-0331$12.50/0

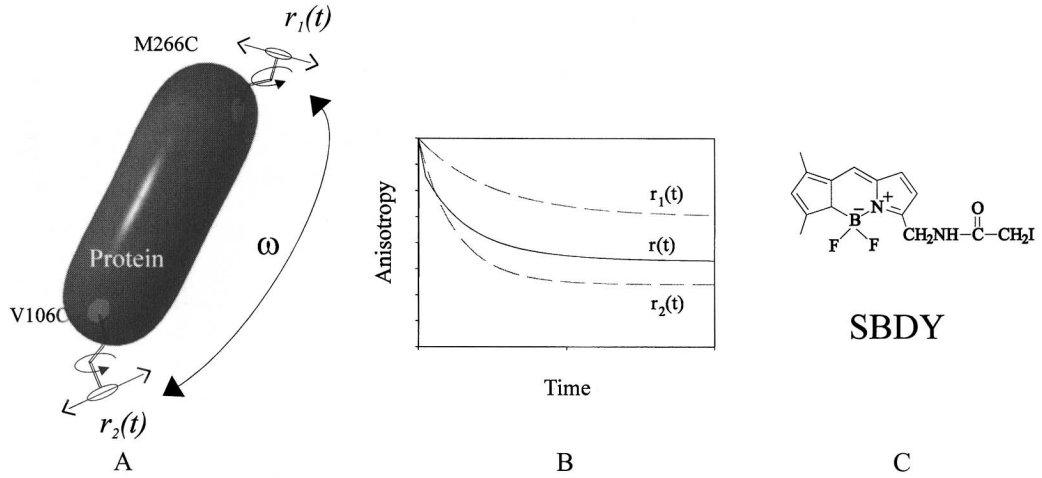

Fig. 1. (A) Schematic of two reorientating *d* molecules located in an immobilized protein. (B) Different contribution to the fluorescence anisotropy. $r_1(t)$ and $r_2(t)$ (----) depend on the local reorientational motions. $r(t)$ is observed for the bichromophoric protein in the presence of energy migration. (C) Structure formulas of *N*-(4,4-difluoro-5,7-dimethyl-4-bora-3a, 4a-diaza-*s*-indacene-3-yl)methyl) iodo-acetamide (SBDY).

fer process within such a bichromophoric molecule is reversible. This case is usually referred to as donor–donor (*dd*) energy migration (DDEM) and it can be studied only by fluorescence depolarization experiments, preferably, fluorescence anisotropy.

Until recently[1,3,4] studies of DDEM between identical fluorophores have been very rare, and usually vitrified samples are examined.[16–18] A likely reason is that, in addition to energy migration, reorientational motions of the *d* molecules will also contribute to the fluorescence anisotropy experiment.

This work aims to present and test a DDEM method for determining intramolecular distances in proteins. To apply the DDEM method, three mutant forms of the protein must be prepared and labeled with carefully selected fluorophores (the double-labeled and the corresponding two single-labeled proteins). The rate of energy migration between the fluorophores within the doubly labeled protein is extracted from the time-resolved fluorescence anisotropy, $r(t)$. The distance between the chromophoric moieties is then calculated from the migration rate. The local reorientational motions of the fluorophores also contribute to $r(t)$, but their contributions are accounted for by determing the corresponding time-resolved anisotropies, $r_1(t)$ and $r_2(t)$, for the single-labeled proteins. In Fig. 1A a schematic picture of a double-labeled protein is given, and the time-resolved fluorescence anisotropy is illustrated in Fig. 1B.

It is desirable to have a sample that contains 100% double-labeled protein, which is sometimes difficult to achieve. Usually, the samples of the double-labeled protein contains fractions of single-labeled proteins. In this work, we investigate the influence of partially labeled proteins on the calculated intramolecular distance when using the DDEM method. The study is performed by generating synthetic fluorescence data which resemble experimental data for the three forms of the studied protein. Data for the partially double-labeled systems were constructed by including different fractions of the two single-labeled protein forms. The synthetic data were then analyzed in the same way as the real experimental data. As a model system we have used the latent form of plasminogen activator inhibitor type 1 (PAI-1), which is a protease inhibitor that belongs to the serpin family of inhibitors. Since PAI-1 lacks cysteine residues, substitution mutants containing one or two unique cysteines for labeling were constructed. After labeling with sulfhydryl specific fluorophores, the mutants reveal biochemical characteristics very similar to those of the wild-type of PAI-1.[1,19,20]

MATERIALS AND METHODS

Fluorescent Probe Molecules

The sulfhydryl-specific derivative of BODIPY, *N*-(4,4-difluoro-5,7-dimethyl-4-bora-3a,4a-diaza-s-indacene-3-yl)methyl) iodo-acetamide (SBDY), was used in this study; see Fig. 1C. SBDY is commercially available from Molecular Probes, Inc., Eugene, OR. The SBDY probe is covalently linked to a cysteine residue in a protein by replacing the I atom in the probe by the S atom of the cysteine residue. The Förster radius (R_0) was de-

termined to be about 60 Å for different labeled single Cys mutants. A scatter in the R_0 values was observed which correlated with varying amounts of I ions remaining from the labeling procedure. The reason for the scattering values is the overlap between the absorption spectra of the ions and BODIPY, which, depending on the ion concentration, will have a different influence on the calculated R_0 value. To avoid this complication we have used $R_0 = 57 \pm 1$ Å [$\langle\kappa^2\rangle = {}^2/_3$], which was obtained previously for various BODIPY derivatives in ethanol.[21] Compared to BODIPY, the absorption and fluorescent spectra of SBDY are slightly red shifted, by about 1 nm. The maximum molar absorptivity in ethanol has been determined to be 80 000 M^{-1} cm^{-1} at 505 nm.

Construction of Expression Plasmids for PAI-1 Cysteine Mutants

The plasmid PDL06, designed for expression of human PAI-1 cDNA[22] in bacteria, was used as the template for site-directed mutagenesis using a commercial *in vitro* mutagenesis kit, the QuickChange site-directed mutagenesis kit (Stratagene, USA). The amino acids Val106 and Met266 were substituted with cysteine. Expression and purification of the PAI-1 cysteine mutants were performed as described previously.[23]

Labeling of the PAI-1 Cysteine Mutants with SBDY

Active purified PAI-1 Cys mutants were converted into latency by incubation at 37°C for 12 h in 50 m*M* sodium phosphate (pH 5.6), 0.1–0.3 *M* $(NH_4)_2SO_4$, 1 m*M* DTT, and 0.02% NaN_3. Complete conversion to latency was confirmed by activity assay.[22] The latent PAI-1 cysteine mutants were concentrated on a HiTrap-heparin column (Pharmacia AB, Sweden) and then desalted on a Sephadex G-25 column (Pharmacia AB) with buffer containing 50 m*M* sodium phosphate (pH 7.2), 150 m*M* sodium chloride, and 1 m*M* EDTA.[20] Subsequently, cysteine residues in the PAI-1 mutants were labeled with a 10–20 times molar excess of SBDY (Molecular Probes, Inc.). The reaction was performed in the dark for 2 h at room temperature, then for 12 h at +4°C.[1,20] The excess of free SBDY was removed by gel filtration on a Sephadex G-25 column in buffer containing 50 m*M* sodium phosphate (pH 7.2), 150 m*M* sodium chloride.[20] The incorporation efficiency was calculated from the molar ratio of SBDY to PAI-1 determined by a spectroscopic method[20] and by using the Micro BCA protein assay kit (Pierce, USA)

Fluorescence Measurements

In order to eliminate the influence of protein rotation on the fluorescence time scale, all samples contained 50% (by volume) of glycerol (BDH; quartz glass distilled). The influence of glycerol is negligible on the activity of PAI-1.[20] For labeled PAI-1 double and single mutants, that is, the double as well as the corresponding single mutants, two independent preparations and fluorescence experiments were performed. The temperature of the samples was kept at 277 ± 0.5 K. To avoid reabsorption, the maximum absorbance was kept below 0.08. The fluorescence spectra and steady-state anisotropies were determined on a SPEX fluorolog 112 instrument equipped with Glan–Thompson polarizers. The excitation and emission bandwidths were set to 5.6 and 2.8 nm, respectively. The mean value of the steady-state emission anisotropy (r_s; excited at 500 nm) was calculated by integration of

$$r_s(\lambda) = \frac{F_{VV}(\lambda) - g(\lambda) F_{VH}(\lambda)}{F_{VV}(\lambda) + 2g(\lambda) F_{VH}(\lambda)}$$

over the region 520 to 560 nm. Here F denotes the fluorescence intensity and the first and the second subscripts indicate the settings [vertical (V) or horizontal (H)] of the excitation and emission polarizers, respectively. The correction factor, $g(\lambda) = F_{HV}(\lambda)/F_{HH}(\lambda)$, compensates for the different transmission efficiencies of vertically and horizontally polarized light, and it was determined from measurements on BODIPY dissolved in ethanol.

The single-photon counting experiments were performed on a PRA 3000 system (Photophysical Research Associates Inc., Ontario, Canada). The excitation source was a thyratron-gated flash lamp (Model 510C; PRA) filled with deuterium gas and operated at ca. 30 kHz. The excitation and emission wavelengths were selected by interference filters (Omega/Saven AB, Sweden) centered at 500 nm (HBW = 12.1 nm) and 550 nm (HBW = 40 nm), respectively. The instrument response function was determined with a light-scattering solution (LUDOX)

The time-resolved fluorescence anisotropy was determined by repeatedly collecting fluorescence decay curves with the excitation polarizer alternating between the parallel [$F_{VV}(t)$] and the horizontal [$F_{HV}(t)$] position, while the emission polarizer was set in the vertical position. The total number of counts, F_{VV}^{tot} and F_{HV}^{tot}, for the polarizer settings $F_{VV}(t)$ and $F_{HV}(t)$ were determined by integration of the intensity over the whole range of the decay curve. From the measured decay curves, a sum

curve,

$$s(t) = F_{VV}(t) + 2KF_{HV}(t)$$

and a difference curve,

$$d(t) = F_{VV}(t) - KF_{HV}(t)$$

were constructed. The scaling factor K was calculated from

$$K = (1 - r_s)(1 + 2r_s)^{-1} F_{VV}^{tot} (F_{HV}^{tot})^{-1}$$

The maximum number of counts in the maximum of the $d(t)$ curves was always about 80,000.

Data Analysis

The experimental difference $[D(t)]$ and sum $[S(t)]$ curves were constructed according to

$$D(t) = \int_0^t E(t - x)r(x)w(x)dx$$

and

$$S(t) = \int_0^t E(t - x)w(x)dx$$

where $E(t - x)$, $r(t)$, and $w(t)$ denote the instrumental response function, fluorescence anisotropy, and photophysics decays, respectively. The photophysics obtained by deconvolution of $S(t)$ was used for deconvoluting $r(t)$ from $D(t)$. For reconvolutions, a nonlinear least-squares analysis was used, based on the Levenberg–Marquardt algorithm. The fitting range over $d(t)$ was about 45 ns, starting from the maximum of the response function. The criterion of fitting is to minimize the sum of squares defined by

$$\chi^2 = \sum_i \left[\frac{D(i) - d(i)}{\sigma(i)}\right]^2$$

where $\sigma(i)$ is the statistical uncertainty of $d(i)$. The variable i indicates a discrete time channel. To ensure that the fitting is reasonable, the steady-state fluorescence anisotropy was calculated from $r(t)$ and $w(t)$ and compared with the experimental value of r_s. The quality of the fit was judged by the global χ^2 value, the χ^2 values calculated for the individual decay curves, and the residual graphs. The calculations were performed on a Silicon Graphics, IRIS INDIGO, workstation equipped with a MIPS R4000 processor.

Synthetic Single-Photon Counting Data

For testing mathematical models that describe fluorescence decays, the criterion is how well one recovers the known decay parameters. By using a model with known parameters, synthetic data can be generated that mimic a perfect experiment. Such data are very valuable for assessing the possibility of distinguishing between different models for a complex decay and for judging the stability of the extracted parameters. In the present work, the data were generated by a Monte Carlo convolution method,[24] which automatically provides the relevant statistics of single-photon counting experiments, i.e., the Poissonian statistics. A brief outline of this method in the context of fluorescence depolarization experiments is given below.

The mathematical expression for the anisotropy, $r(t)$, describing energy transfer in bichromophoric molecules, depends on a set of parameters. Knowing these parameters, the polarized fluorescence decays $I_{VV}(t)$ and $I_{HV}(t)$ are constructed according to

$$I_{VV}(t) = [1 + 2r(t)]w(t)$$

$$I_{HV}(t) = [1 - r(t)]w(t)$$

The fluorescence decays $F_{VV}(t)$ and $F_{HV}(t)$ in experiments are convolutions of the true decay functions $I_{VV}(t)$ and $I_{HV}(t)$ with the normalized instrumental response function $[E(t)]$:

$$F_{VV}(t) = \int_0^t E(t - \tau)I_{VV}(\tau)d\tau$$

$$F_{HV}(t) = \int_0^t E(t - \tau)I_{HV}(\tau)d\tau$$

In the Monte Carlo convolution method two random numbers, X_E and X_I, are generated to follow the density functions $E(t)$ and $I_{AV}(t)$ ($A = V$ or H), respectively. Two kinds of random number generators were used, one for generating a uniform distribution of numbers between 0 and 1 and the second for generating discrete random numbers of a specific distribution. We used the uniform pseudo-random number generator of Marsaglia and Zaman[25] and the alias method[26] to convert the uniform distribution into discrete random numbers. The sum of X_E and X_I represents the time for one emission event. By generating many emission events, a histogram can be constructed which is the discrete function $F_{AV}(t)$ given by the convolution integral above. The instrumental response function, $E(t)$, was taken to be a Gaussian distribution with the same full width at half-maximum as

that of the experimental response function, that is, about 1.5–2 ns. The time resolution was 0.18 ns/channel. In order to minimize the roundoff errors inherent in this method, each channel was split into 32 subchannels that were summed after the random convolution. The number of counts in each decay was the same as in real experiments. From the generated decay curves the steady-state fluorescence anisotropy was calculated from

$$r_s = \frac{\int_0^\infty r(t)w(t)dt}{\int_0^\infty w(t)dt}$$

The synthetic decay data were then analyzed using the procedure described under Data Analysis.

RESULTS AND DISCUSSION

Model

In the model presented below it is assumed that the photophysics of each *d* molecule within a pair is the same. In practice however, the photophysics of many fluorescent probes is more or less sensitive to the polarity, the pH, and the presence of quenching molecules. These properties may, of course, differ considerably between different regions of a protein. Consequently, the choice of fluorescent label is important. We have found that derivatives of the recently developed fluorophore, 4,4-difluoro-4-borata-3a-azonia-4a-aza-*s*-indacence (BODIPY), meet this, as well as other important criteria, very well.[21] The fluorescence lifetime of the probe is about 5.5 ns, and it is independent of pH over a large range and changes very little with solvent polarity. However, both Trp and Tyr quench BODIPY with quenching constants of about 15 M^{-1}. Therefore, when labeling a protein molecule at different positions, it is necessary to examine the photophysics decay for each choice of site.

The time-resolved fluorescence anisotropy, $r(t)$, is an orientational correlation function that correlates the orientation of the excited molecules (given by eulerian angles Ω_0 and Ω) at the times of excitation ($t = 0$) and emission ($t = t$). The rotation of an excited molecule and the excitation energy migration contribute to $r(t)$. We assume that the orientational correlation functions $[r_i(t)]$ and the excitation probability $[p(t)]$ of the two identical *d* molecules can be separated[3] and that the fluorescence anisotropy can be written as:

$$r(t) = \frac{1}{2}[r_1(t) + r_2(t)]\,p(t) + \frac{1}{2}[r_{12}(t) + r_{21}(t)]\,[1 - p(t)] \quad (1)$$

Here $r_{ij}(t)$ denotes contributions due to energy migration from the initially excited d_i molecule to its neighbor d_j. The reorientational motions of the *d* molecules attached to a macromolecule, like a protein, are of global and local nature. The local mobility is illustrated schematically in Fig. 1A, where each *d* molecule can undergo anisotropic rotations relative to the macromolecule. The overall tumbling of the protein molecule is neglected in the following (see Results and Discussion). As described by Johansson *et al.*[3] and Karolin *et al.*,[4] the modeling of $r_j(t)$ and $r_{ij}(t)$ can be summarized by the following equations:

$$r_i(t) = \frac{2}{5}\{(1 - \rho_i^\infty)\gamma_i(t) + \rho_i^\infty\} \quad (2)$$

$$r_{ij}(t) = \frac{2}{5}\{(\rho_{ij}^0 - \rho_{ij}^\infty)\gamma_i(t) + \rho_{ij}^\infty\} \quad (3a)$$

$$r_{ij}(t_\infty) = \frac{2}{5} D_{00}^{(2)}(\delta)\,\langle D_{00}^{(2)}(\Omega_{D_iM_i})\rangle \quad (3b)$$

$$\langle D_{00}^{(2)}(\Omega_{D_jM_j})\rangle \equiv \frac{2}{5}\rho_{ij}^\infty$$

In Eq. (2) $\rho_i^\infty = \langle D_{00}^{(2)}(\Omega_{M_i D_i})\rangle$ and $\langle D_{00}^{(2)}(\Omega_{M_i D_i})\rangle$ is a second-rank order parameter which describes the local order of the transition dipole moment (M) of the ith donor with respect to an effective orientation axis (D_i) in the protein. The order parameter can take any value between -0.5 and 1. In Eq. (3b), $\gamma_i(t)$ is a sum of exponential functions and δ denotes the angle between the orientation axes D_i and D_j.

The excitation probability of the initially excited donor $[p(t)]$ within a *dd* pair is, in the dynamic and slow limits, easily obtained from the master equation of DDEM within the pair, which is given by

$$p(t) = \frac{1}{2}\{1 + \exp(-2\omega t)\} \quad (4a)$$

where

$$\omega = \frac{3}{2}\langle\kappa^2\rangle\left(\frac{R_0}{R}\right)^6 \tau^{-1} \quad (4b)$$

The fluorescence lifetime, the Förster radius, and the intramolecular distance are denoted τ, R_0, and R, respectively. The average angular dependence of dipole–dipole coupling in the dynamic limit is denoted $\langle\kappa^2\rangle$. To model the orientational dependence of $\langle\kappa^2\rangle$, we use:[4,27]

Table I. The Studied Forms of PAI-1 are the Double Mutant V106C-M266C and the Corresponding Single Mutants V106C and M266C[a]

Mutant	r_s	ϕ (ns)	$r(0)$	ρ^0	$r(t_\infty)$	$\langle D^{(2)}_{00}(\Omega_{DM})\rangle$	$\omega \times 10^{-9}$ s^{-1}	$\langle\kappa^2\rangle$	δ (°)	R (Å)	R_c (Å)
V106C	0.299	10.4 ± 2.1	0.332		0.236	0.80					
M266C	0.302	11.4 ± 2.0	0.333		0.239	0.80					
V106C-M266C	0.221		0.208	0.379	0.126		0.45 ± 0.1	1.31	52	54 ± 3.0	55.1

[a]The mutants were labeled with the fluorophore SBDY, which is connected to the protein with a linker. The steady-state fluorescence anisotropy (r_s), rotational correlation time (ϕ), initial anisotropy [$r(0)$], residual anisotropy [$r(t_\infty)$], rate of energy migration (ω), order parameter ($\langle D^{(2)}_{00}(\Omega_{DM})\rangle$), $\langle\kappa^2\rangle$, δ^0 (see text), and intramolecular distance (R) are presented. The errors indicated represent arithmetic mean values of two independent experiments. The errors of all parameters, except ϕ, ω, and δ^0, are within ±4%. The distance (R) between the *dd* molecules is calculated from the migration rate (ω) by using the average square angular dependence of dipole–dipole coupling ($\langle\kappa^2\rangle$). The R value is compared with the distance between the C_α carbon of the mutated amino acid (R_c), obtained from the crystal structure of latent PAI-1.

$$\langle\kappa^2\rangle = \frac{2}{3} + \frac{2}{3}\langle D^{(2)}_{00}(\Omega_{D_iM_i})\rangle + \frac{2}{3}\langle D^{(2)}_{00}(\Omega_{D_jiM_j})\rangle D^{(2)}_{00}(\delta) + 2\langle D^{(2)}_{00}(\Omega_{D_iM_i}) D^{(2)}_{00}(\Omega_{D_jiM_j})\rangle D^{(2)}_{00}(\delta) \quad (5)$$

Note that all parameters in Eq. (5) are available from the residual anisotropies obtained for each *d* molecule and the *dd* pair.

Contributions to $r(t)$ in the case of *partial labeling* of the bichromophoric protein is accounted for by the following equation:

$$r(t) = \frac{1}{2}[(r_1(t) + r_2(t))p(t) + (r_{21}(t) + r_{21}(t))(1 - p(t))](1 - (f_1 + f_2)) + r_1(t)f_1 + r_2(t)f_2 \quad (6)$$

The application of Eq. (6) to data analysis involves two more parameters compared to Eq. (1), which likely reduces the stability of the extracted parameters. This question is examined below.

Mono- and Bilabeled Cys Mutants of PAI-1

Substitution mutants of latent PAI-1 containing one or two cysteine residues were constructed using site-specific mutagenesis, as described under Materials and Methods. We have studied the single mutants V106C and M266C, as well as the double mutant V106C-M266C. The SBDY probe was covalently bound to the cysteine residues of the mutants. To eliminate the influence of rotation of the protein molecules on the fluorescence anisotropy, all solutions contained 50% (by volume) of glycerol. The fluorescence decay of all mutants is found to be nearly monoexponential, with a dominating lifetime (>90%) of about 5.3 ns.

Intramolecular Order and Reorientation

Time-resolved fluorescence anisotropy of the labeled PAI-1 single mutants gives information on the local rotational rates of the fluorescent group, as well as on its local orientational restriction, or order [ρ_i^∞; see Eq. (2)]. The decay of $r_i(t)$ can be obtained from the difference curve by fitting with one rotational correlation time (ϕ_i) and a static term (ρ_i^∞) according to Eq. (2). The rotational correlation times and the residual anisotropies are very similar in the two studied sites, V106C and M266C; see Table I. The rather high value for the limiting anisotropies [i.e., $r(t_\infty) \cong 0.23$] implies that the order parameters must take positive values, i.e., $\langle D^{(2)}_{00}(\Omega)\rangle > 0.5$. Furthermore, the large values of the order parameters (see Table I) mean that the local orientational restrictions of the BODIPY moieties are high. The initial anisotropy values $\{r(0)\}$ were found to be smaller than the limiting anisotropy value of $r_0 = 0.37$.[21] This strongly suggests a small influence from rapid motions of the BODIPY moiety, such as librational or rotational motions (10^{-12} to 10^{-11} s) which are beyond the time resolution of the experimental equipment. Taken together, the $r_1(t)$ and $r_2(t)$ data suggest that the local environments of the probes are very similar.

Intramolecular Distances

To analyze the $r(t)$ data obtained for the labeled double mutants of PAI-1, we assume that the rates and restrictions of local motions are very similar to those of the corresponding single mutants. This assumption is supported by the fact that the probes are localised far away from each other in the protein structure and that the formation of the Cys mutant and its labeling do not have any significant influence on the inhibitory activity. In these circumstances the strategy of global analysis[28,29] could be applied. In the application to DDEM this means that, for each of the models presented above

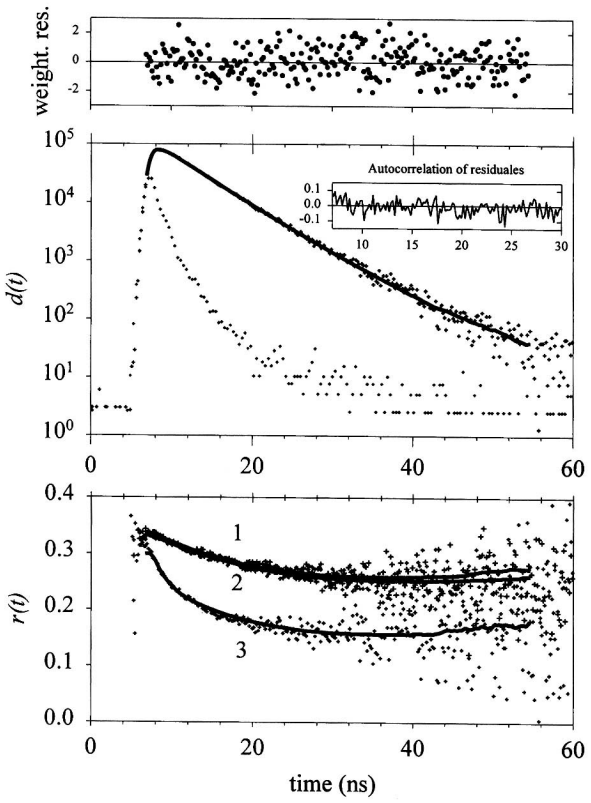

Fig. 2. Example of decay curves obtained for the latent PAI-1 V106C-M266C system labeled with SBDY. The upper graph shows the fitted difference curve of the double mutant together with the weighted residuals. The lower graph shows the anisotropy decay for (1) M266C, (2) V106C, and (3) V106C-M266C. The $r(t)$ curves were constructed by dividing the $d(t)$ and $s(t)$ decay curves. Consequently they do not represent the true shape of $r(t)$ since the response function has a width at half-full maximum of about 2 ns.

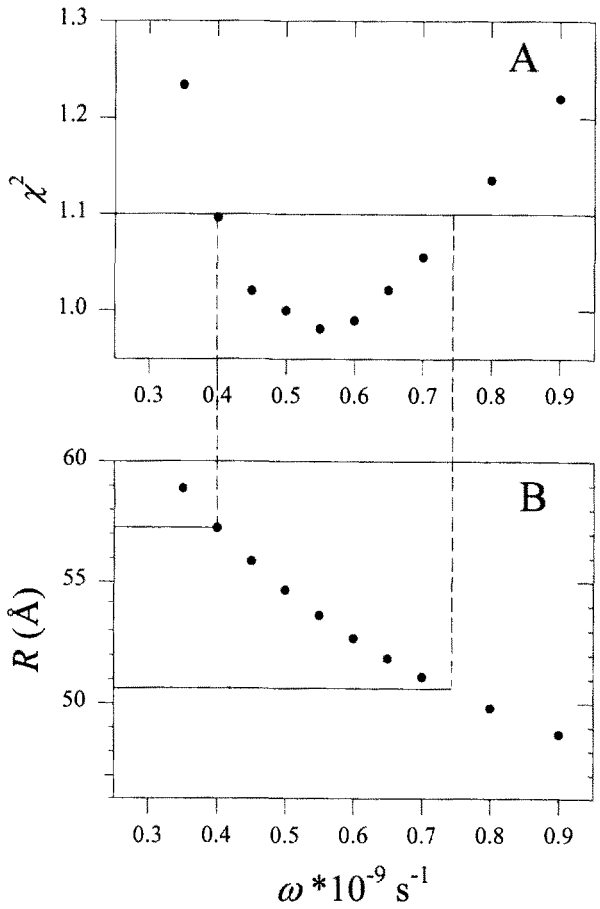

Fig. 3. (A) The χ^2 parameter plotted as a function of the transfer rate (ω) obtained from the analysis of the double mutant V106C-M266C; see Fig. 1. The transfer rate was fixed to the indicated value. (B) The calculated distances corresponding to the different transfer rates. The minimum of the χ^2 graph corresponds to a distance of about 54 Å. If any χ^2 value lower than 1.1 is considered as an acceptable fit, the distance can be estimated to be 54 ± 3 Å. This value is in excellent agreement with the distance of 55.1 Å obtained from the X-ray structure.

[i.e., Eqs. (1)–(6)], data obtained for the two single mutants and the double mutant of PAI-1 are simultaneously fitted to Eqs. (1)–(5) or Eqs. (2)–(6). The experimental and fitted anisotropy and difference curves are shown in Fig. 2. For the PAI-1 mutants studied here, it proved sufficient to use one rotational correlation time. The analysis of the data set gives a value on the rate of energy migration, as well as order parameters. By using these values and Eqs. (4b) and (5), the intramolecular distance (R) can be calculated (see Table I). The R values given in Table I were obtained for two independent preparations and experiments. To examine the quality of the analysis, the χ^2 test parameter was plotted as a function of different fixed values on the migration rate (see Fig. 3A). As shown in Fig. 3B, the minimum of χ^2 corresponds to about 54 Å. For comparison, the distance (R_c) between the two C_α atoms corresponding to mutated amino acid residues in the PAI-1 double mutant is 55.1 Å as obtained from the crystal structure of the wild-type latent PAI-1.[30] There is a good agreement between R and R_c, indicating that the linker is adopting a rather nonextended conformation, which is in excellent agreement with previous findings.[4]

Influence of Partial Labeling

When determining the intramolecular distance in a protein by the DDEM method and Eqs. (1)–(5), it is assumed that the double mutants are 100% labeled. However, assume that the degree of labeling is lower, say, 80% for the double mutant and 90% for each of the single mutants. It is then relevant to ask whether one can

Table II. Reanalysis of Synthetic Fluorescence Anisotropy Data for Different Mixtures of Double (M266C-V06C) and Single (M266C, V106C) Mutants of PAI-1 Labeled with SBDY[a]

	Recovered parameter									
	Not including fractions in the DDEM model					Including fractions in the DDEM model				
f (%)	$\omega\times10^9$ s^{-1}	ρ^0	δ (°)	$\langle\kappa^2\rangle$	R (Å)	$\omega\times10^9$ s^{-1}	ρ^0	δ (°)	$\langle\kappa^2\rangle$	R (Å)
10	0.565	0.480	44	1.70	55.5	0.565	0.372	51	1.36	53.5
20	0.547	0.589	38	2.02	57.4	0.548	0.373	52	1.34	53.6
40	0.481	0.797	20	2.73	61.7	0.481	0.338	50	1.44	55.5
45	0.582	0.860	14	2.89	60.3	0.574	0.386	52	1.33	53.2

[a]The fraction of each single mutant, f, is taken to be the same. Thus, f = 10% means that the fraction of double mutant is 80%. Data were synthesized with the following parameters: $\omega = 0.535 \cdot 10^9$ s^{-1}, $\rho^0 = 0.368$, $\delta = 51°$, and $\langle\kappa^2\rangle = 1.35$, which corresponds to 53.9 Å. From the crystal structure of the latent PAI-1[30], the distance between the C_α atoms in the backbone was determined to be 55.1 Å. The reanalysis was performed either by neglecting [see Eqs. (1)–(5)] the fractions, thus treating a sample as being 100% labeled, or by including [see Eqs. (2)–(6)] the fractions.

still analyze such data? For this, the extended model given by Eq. (6) was applied, where the fluorescence anisotropy accounts for mixtures of single- and double-labeled proteins. Moreover, how does 90% instead of the expected 100% influence the calculated distance when using the simple model? To answer these questions synthetic data were generated for the experimental parameters obtained from studies of the V106C, M266C, and V106C-M266C mutants. Data were generated for the double mutant mixed with varying mole fractions (f) of the single mutants. These data were then reanalyzed using both of the models, i.e., accounting for and neglecting partial labeling. As shown in Table II, the extended model recovers the true parameters remarkably well, even if only 10% of the double-labeled mutant is present in the sample. Compared to the extended model, the results of the crude model are much worse. However, the crude model still gives acceptable R values for 60 mol% of the double-labeled mutant, provided that one can accept a 20% deviation from the true distance. In the present work, the method used to determine the degree of labeled V106C-M266C mutant does not allow us to discriminate between 90 and 100% labeling. We also find that, independent of the model used to analyze the data, the distance extracted is 54 ± 3 Å. It is thus tempting to state that a 90% degree of labeling is sufficient to extract good distance values even using the crude model. However, we think it is advisable always to generate synthetic data for each particular system studied, since this offers great possibilities to check carefully the stability of different parameters.

Conclusions

It is possible to prepare fluorophore-labeled single and double mutants of the plasminogen activator inhibitor-1 (PAI-1) in its latent conformation. The fluorophore SBDY shows very similar photophysics in different cysteine mutants of PAI-1.

The method described may be a powerful tool for determining conformation changes in proteins. For example, we have used this method to study molecular details in the inhibition of a target protease by PAI-1.[2]

By analyzing synthetic data generated within the anisotropy model, one can assess the quality of the extracted parameters. Moreover, the effects on the extracted parameters which result from having mixtures of partially labeled double mutants can be conveniently investigated. The model and methods presented for analyzing fluorescence anisotropy data predict intramolecular distances which are in good agreement with independently determined values.

ACKNOWLEDGMENTS

We are grateful to Malgorzata Wilczynska and Ming Fa for helpful discussions. This work was supported by the Swedish Natural Research Council (Grants NFR K-AA/KU 08676-308 and NFR B-AA/BU 08473-311)

REFERENCES

1. S. B. Aleshkov, M. Fa, J. Karolin, L. Strandberg, L. B.-Å. Johansson, M. Wilczynska, and T. Ny (1996) *J. Biol. Chem.* **271**, 21231–21238.
2. M. Wilczynska, M. Fa, J. Karolin, P.-I. Ohlsson, L. B.-Å. Johansson, and T. Ny (1997) *Nature Struct. Biol.* **4**, 354–357.
3. L. B.-Å. Johansson, F. Bergström, P. Edman, I. V. Grechishnikova, and J. G. Molotkovsky (1996) *J. Chem. Soc. Faraday Trans.* **92**, 1563–1567.

4. J. Karolin, M. Fa, M. Wilczynska, T. Ny, and L. B.-Å. Johansson (1998) *Biophys. J.* **74**, 11–21.
5. T. Förster, (1948) *Ann. Phys.* **2**, 55–75.
6. M. N. Berberan-Santos, and B. Valeur, (1991) *J. Chem. Phys.* **95**, 8048–8055.
7. M. Kaschke, N. P. Ernsting, B. Valeur, and J. Bourson (1990) *J. Phys. Chem.* **94**, 5757–5761.
8. S. A. Latt, H. T. Cheung, and E. R. Blout (1965) *J. Am. Chem. Soc.* **87**, 995–1003.
9. B. W. Van Der Meer, G. I. Coker, and S.-Y. S. Chen (1994) *Resonance Energy Transfer Theory and Data*, VCH.
10. L. Stryer and R. P. Haugland (1967) *Proc. Natl. Acad. Sci. USA* 719–726.
11. B. Valeur (1989) *Intramolecular Excitation Energy Transfer in biochromophoric Molecules—Fundamental Aspects*, Polonium Press, New York.
12. B. Valeur, J. Muggier, J. Pouget, J. Bourson, and F. Santa (1989) *J. Phys. Chem.* **87**, 6073–6079.
13. J. J. H. Lakey, D. Baty, and F. Pattus (1991) *J. Mol. Biol.* **218**, 639–653.
14. R. P. Haugland (1996) *Handbook of Fluorescent Probes and Research Chemicals*, 6th ed., Molecular Probes, Eugene, OP.
15. E. Stratikos, and P. G. W. Gettins (1997) *Proc. Natl. Acad. Sci. USA* **94**, 453–458.
16. T. Ikeda, B. Lee, S. Kurihara, S. Tazuke, S. Ito, and M. Yamamoto (1988) *J. Am. Chem. Soc.* **110**, 8299–8304.
17. P. I. H. Bastiaens, S. G. Mayhew, E. M. O'Nualláin, A. van Hoek, and A. J. W. G. Visser (1991) *J. Fluoresce.* **1**, 95–103.
18. B. Kalman, A. Sandström, L. B.-Å. Johansson, and S. (1991) *Biochemistry* **30**, 111–117.
19. L. Strandberg, J. Karolin, L. B.-Å. Johansson, M. Fa, S. Aleshkov, and T. Ny (1994) *Res. Thromb.* **76**, 253–267.
20. M. Fa, J. Karolin, S. Aleshkov, L. Strandberg, L. B. A. Johansson, and T. Ny (1995) *Biochemistry* **34**, 13833–13840.
21. J. Karolin, L. B.-Å. Johansson, L. Strandberg, and T. Ny (1994) *J. Am. Chem. Soc.* **116**, 7801–7806.
22. D. Lawrence, L. Strandberg, T. Grundström, and T. Ny (1989) *Eur. J. Biochem.* **186**, 523–533.
23. J.-O. Kvassman and J. D. Shore (1995) *Fibrinolysis* **9**, 215–221.
24. N. C. Fahmida, S. K. Zbigniew, and M. D. Barkley (1991) *Rev. Sci. Instrum.* **62**, 47–52.
25. G. Marsaglia and A. Zaman (1987) Toward a Random Number Generator, Florida State University Report, Gainesville.
26. R. A. Kronmal and A. V. Peterson, Jr. (1979) *Am. Stat.* **33**, 214–218.
27. L. B.-Å. Johansson, P. Edman, and P.-O. Westlund (1996) *J. Chem. Phys.* **105**, 10896–10904.
28. J. R. Knutson, J. M. Beechem, and L. Brand (1983) *Chem. Phys. Lett.* **102**, 501–507.
29. J.-E. Löfroth (1985) *Eur. Biophys. J.* **13**, 45–58.
30. J. Mottonen, A. Strand, J. Symersky, R. M. Sweet, D. E. Danley, K. F. Geoghegan, R. D. Gerard, and E. J. Goldsmith (1992) *Nature* **355**, 270–273.